Article

Direct Observation of Subunit Exchange along Mature Vimentin Intermediate Filaments

Bernd Nöding,[1,2] Harald Herrmann,[3] and Sarah Köster[1,2,*]
[1]Institute for X-Ray Physics, Georg-August-Universität Göttingen, Göttingen, Germany; [2]Center for Nanoscale Microscopy and Molecular Physiology of the Brain, Göttingen, Germany; and [3]Division of Molecular Genetics, German Cancer Research Center, Heidelberg, Germany

ABSTRACT Actin filaments, microtubules, and intermediate filaments (IFs) are central elements of the metazoan cytoskeleton. At the molecular level, the assembly mechanism for actin filaments and microtubules is fundamentally different from that of IFs. The former two types of filaments assemble from globular proteins. By contrast, IFs assemble from tetrameric complexes of extended, half-staggered, and antiparallel oriented coiled-coils. These tetramers laterally associate into unit-length filaments; subsequent longitudinal annealing of unit-length filaments yields mature IFs. In vitro, IFs form open structures without a fixed number of tetramers per cross-section along the filament. Therefore, a central question for the structural biology of IFs is whether individual subunits can dissociate from assembled filaments and rebind at other sites. Using the fluorescently labeled IF-protein vimentin for assembly, we directly observe and quantitatively determine subunit exchange events between filaments as well as with soluble vimentin pools. Thereby we demonstrate that the cross-sectional polymorphism of donor and acceptor filaments plays an important role. We propose that in segments of donor filaments with more than the standard 32 molecules per cross-section, subunits are not as tightly bound and are predisposed to be released from the filament.

INTRODUCTION

Cell mechanics are in great part governed by complex networks of proteins. The so-called cytoskeleton consisting of actin filaments, microtubules, and intermediate filaments (IFs) is fundamentally important for the generation of specific shapes and mechanical properties of the various types of cells in metazoan organisms (1,2). These physical properties are supposed to be widely modulated by a huge set of associated cross-bridging and motor proteins as well as separate structural entities such as focal adhesions, desmosomes, and other types of junctions (3).

IF proteins display a great genetic variability across cell types and organisms. Nevertheless, they share a common structural plan and common traits (for review, see Parry and Steinert (4) and Herrmann and Aebi (5)). The observed extensive amino-acid sequence variability is supposed to be in part responsible for the establishment of cell type- and tissue-specific mechanical properties (6–10). IF monomers consist of an α-helical rod domain flanked by flexible, mostly nonstructured non-α-helical amino-terminal (head) and carboxy-terminal (tail) domains. After reconstitution from denaturing solutions into low salt buffers, cytoplasmic IF proteins such as vimentin form stable tetramers that consist of two coiled-coil dimers in a half-staggered antiparallel orientation. By raising the ionic strength, typically eight tetramers laterally assemble to form a unit-length filament (ULF). Subsequently, these ULFs longitudinally anneal and form extended filaments (Fig. 1 *a*). In the case of the mesenchymal proteins desmin and vimentin, filaments have been demonstrated to radially compact, in a third phase of the assembly process, by a few nanometers (11–13). This step occurs within the first 10 min of assembly. The spatial organization of the tetrameric complexes within filaments as well as filament precursors has been investigated by small-angle x-ray scattering (14,15). Moreover, employing quantitative electron microscopy methods and mathematical modeling, the assembly kinetics have been established for vimentin (16–18).

The hierarchical self-assembly from tetrameric complexes to filaments with several subunits per cross-section that are laterally associated is characteristic of IFs and distinguishes them from the other cytoskeletal filaments. This distinct assembly mechanism gives rise to repetitive interaction sites of the individual coiled-coils with one another within a given filament segment due to periodically alternating acidic and basic charge clusters (4,19). This is in strong contrast to actin filaments and microtubules that are made from globular proteins that associate in a polar and nucleotide-dependent fashion, leading to very dynamic filaments. As a consequence of the structural principle of a lateral alignment of fibrous subunits, IFs can be stretched approximately a factor of 3 in length (20) and at the same time they are practically insoluble under physiological conditions as well as in buffers of high ionic strength and nonionic detergents (21).

Submitted June 2, 2014, and accepted for publication September 9, 2014.

*Correspondence: sarah.koester@phys.uni-goettingen.de

Editor: Jochen Guck.

0006-3495/14/12/2923/9 $2.00

http://dx.doi.org/10.1016/j.bpj.2014.09.050

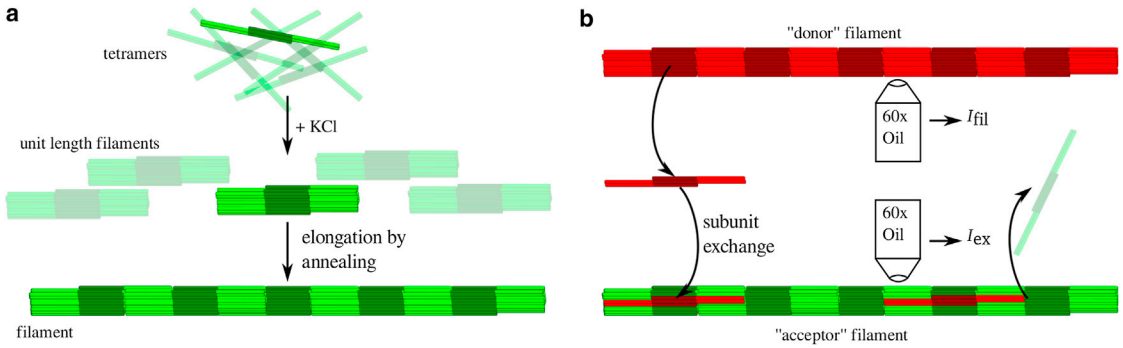

FIGURE 1 Schematics of different mechanisms of subunit incorporation into IFs. (*a*) Assembly of vimentin IFs occurs in a distinct hierarchical manner. Eight tetramers align laterally to form a unit-length filament (ULF). ULFs attach end-to-end and thus elongate into filaments. (*b*) Subunits (*illustration* shows tetramers) detach from a filament and enter the soluble pool. Subunits from this pool are again incorporated into filaments. The two colors represent different fluorescent labels used to examine the exchange process. To quantify the subunit exchange process, we determine the ratio A of I_{fil}, the total red fluorescence, and I_{ex}, the red fluorescence colocalized with green filaments. To see this figure in color, go online.

Interestingly, in vimentin filaments the number of monomers per cross-section can deviate significantly from the standard configuration of 32 (i.e., 8 tetramers) monomers both with filaments directly isolated from cells and those reconstituted from isolated proteins (22–25). Hence, IFs are open structures—in sharp contrast to actin filaments and microtubules (11,23). Depending on the ionic conditions used for assembly, i.e., in particular in the presence of magnesium ions, the number of monomers can rise to 84. However, under physiological conditions, values reach only up to 48 monomers per cross-section. Because of the assembly mechanism, mini-filaments, i.e., ULFs, of different mass can longitudinally anneal and therefore even along one and the same filament, segments with low number of monomers may alternate with those having a higher number (11,13).

This polymorphism in cross-section opens up the possibility for a dynamic subunit exchange of fully assembled filaments along their whole length (see Fig. 1 *b* for a suggested mechanism). For IFs within living cells, such a process was first suggested for vimentin IFs (26), where chicken vimentin was expressed in mouse fibroblasts, and immunofluorescence as well as immunoelectron microscopy were employed to investigate the incorporation of the newly synthesized vimentin. Following similar experimental strategies, the dynamics of intracellular networks have been investigated (27). In a next step, fluorescence-recovery-after-photobleaching experiments were performed to directly visualize the exchange of GFP-labeled vimentin subunits within IFs with soluble GFP-vimentin complexes (28). Using labeled versions of vimentin and neurofilament proteins, the potential of subunit exchange between IFs in vivo was further investigated (29).

Cell fusion experiments in combination with photobleaching methods and photoactivatable fluorescent fusion-proteins were used to demonstrate that filaments anneal end-to-end in vivo, too, and "intercalary subunit" exchange does indeed occur. In cellular systems, phosphorylation of the IF head domain, mediated by different kinases, is thought to lead to disassembly of filaments into tetramers and thus regulates the equilibrium between the soluble pool of tetramers and the filament network (30). This process is especially relevant in cell division, as phosphorylation at distinct sites in the head domain may lead to the entire disassembly of IF networks (Chou et al. (31) and references therein). In vitro, subunit exchange has not been directly observed for vimentin filaments. In particular, when filaments containing two kinds of fluorescently labeled vimentin were mixed after 1 h of assembly and allowed to further assemble for up to 48 h, the end-to-end annealing of these red and green filaments was immediately evident by total-internal-reflection fluorescence microscopy. By contrast, subunit exchange between individual filaments was not detected to occur to a significant degree with the employed observation technique, in particular at the specific sensitivity used for demonstrating the head-to-tail association of long, mature filaments with each other (18).

For vimentin, it has been shown that the assembled filaments are uniform in diameter when the tetramers are dialyzed into the assembly buffer. However, upon direct mixing with concentrated assembly buffer, a pronounced polymorphism is observed in which neighboring segments in a filament may contain as few as four or as many as 12 tetramers per cross-section (11). This type of structural organization harbors various sites of imperfections, and therefore this polymorphic structural organization could be the cause for enhanced subunit exchange. This inherent property of IFs has long been recognized and pointed out as a potential functional property of various IF systems (32).

Following the notion of subunit exchange in IFs and modifying the experimental strategies from the cell experiments accordingly, we here investigate the phenomenon further by studying fluorescently tagged vimentin using a sensitive data analysis method. We find that soluble subunits are indeed incorporated into fully assembled filaments over time. Immediately after adding soluble tetramers, the

incorporation proceeds quickly but slows down after ~1 h, which coincides with the equilibrium reached in the assembly reaction. We thus hypothesize that two competing reactions are occurring: the lateral assembly of tetramers to octamers, 16-mers, and ULFs, followed by longitudinal annealing of ULFs, and the incorporation of tetramers (or larger subunits) into fully assembled filaments.

MATERIALS AND METHODS

Protein preparation and labeling

Human vimentin is expressed in *Escherichia coli* bacteria and purified from inclusion bodies. We investigate a human vimentin mutant with an additional cysteine at its C-terminus and the sole cysteine in the rod domain replaced by alanine. The protein is stored at −80°C in a solution of 8 M urea, 10 mM methyl ammonium chloride, 5 mM Tris-HCl (pH 7.5), 1 mM EDTA, 1 mM DTT, and 0.1 mM EGTA (33).

The point mutations allow us to label the protein via maleimide chemistry without having the fluorophore strongly interfering with filament assembly. We use two fluorescent dyes, AlexaFluor 488 (Invitrogen, Darmstadt, Germany) and Atto 647N (Atto-Tec, Siegen, Germany). The labeling reaction is carried out in 20 mM phosphate buffer at pH 7.0 (18). Nonspecifically bound and free dye is removed from the protein solution by adding L-cysteine at a final concentration of 0.1 M and subsequent column chromatography. Labeled/unlabeled protein is chosen such that 15% of the total protein carries a dye molecule. Thus, if we assume a random distribution of dye molecules, 48% of all tetramers have at least one label attached. At this label ratio, we observe a slightly reduced assembly speed for fluorescently labeled vimentin when compared to unlabeled wild-type protein.

Before assembly, the protein is dialyzed into 2 mM phosphate buffer, pH 7.5 in three steps (6 M urea and two steps without urea) using dialysis membranes with a 50-kDa molecular mass cutoff. Dialysis is performed separately for the differently labeled proteins. To evaluate the exchange of filament subunits, we use three filament types: 1), ATTO 674N (red) labeled filaments, 2), AlexaFluor 488 (green) labeled filaments assembled by dialysis, and 3), AlexaFluor 488 (green) labeled filaments assembled in a reaction tube by addition of KCl to 100 mM.

Microfluidic flow chambers

In situ assembly is performed in microfluidic diffusion chambers (34) that are fabricated from PDMS (polydimethylsiloxane) (Sylgard 184; Dow Corning, Wiesbaden, Germany) using soft-lithography methods (35). Briefly, SU8 3025 resist is spin-coated onto a silicon wafer at a final speed of 3000 rpm and exposed through a quartz glass mask with chrome structure at a wavelength of 365 nm. After development of the resist, this master structure is used to produce the PDMS positive for the microfluidic device. Finally, holes for tubing are punched into the PDMS and the device is completed by sealing with a glass slide. Typically we choose chambers with a diameter of 200 μm and a height of 25 μm. These chambers are connected to a main channel, which is used to supply coating agents, salts, or proteins to the chambers, by a small channel with dimensions of 10 × 10 μm. The device design is shown in Fig. 2 and the inset shows the chambers.

To prevent adhesion of the vimentin to the channel walls, we apply a lipid bilayer coating to the surfaces. To this end, we assemble the device by plasma-cleaning the structured PDMS and a glass slide, and bringing them into contact to form a tight bond. Immediately afterwards we coat the channel walls with a mixture of 98% DOPC (1,2-dioleoyl-*sn*-glycero-3-phosphocholine; Avanti, Alabaster, AL) and 2% DHPC labeled with Texas Red (1,2-diheptanoyl-*sn*-glycero-3-phosphocholine; Invitrogen, Darmstadt, Germany) for quality control (36,37). The lipid solution is sonicated with a probe sonicator to obtain small unilamellar vesicles. The device is connected to gas-tight syringes (Hamilton, Reno, NV) actuated by Nemesys syringe pumps (Cetoni, Korbussen, Germany) with polyethylene tubing (Intramedic PE20; BD, Franklin Lakes, NJ). Lipid solution is flushed through the main channel of the device. The flow rates are set to 50 μL/h. The spreading of the vesicles into a bilayer on the chamber walls is monitored by fluorescence microscopy and is finished after ~30 min. The lipid bilayer remains intact for at least 24 h, when air is excluded.

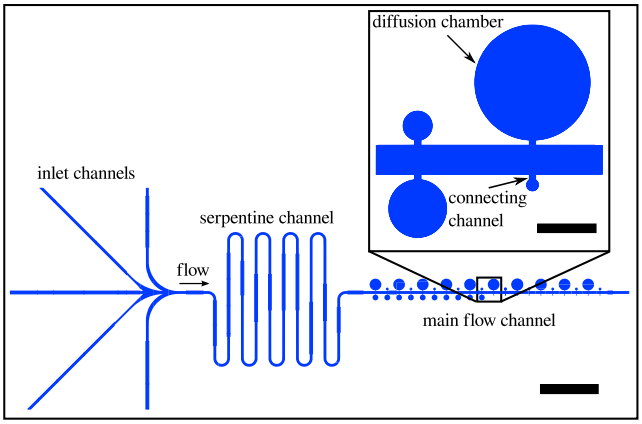

FIGURE 2 Geometry of the microfluidic device (scale bar, 1 mm). (*Left-hand side*) The five inlets are used to combine components at defined mixing ratios; the long serpentine channel that follows downstream ensures that the components are well mixed before they enter the main channel (to the *right*); diffusion chambers are connected to the main channels via small channels that allow mostly for diffusion, but not for considerable flow. Using this setup, we can exchange the buffer within the diffusion chambers without perturbing filament assembly by flow (i.e., similar to dialysis), and concomitantly observe the IFs using a microscope. (*Inset*) Diffusion chambers (scale bar, 100 μm). To see this figure in color, go online.

Microscopy

Confocal microscopy images (105.5 × 105.5 μm^2 or 211 × 211 μm^2, 1024 × 1024 $pixels^2$) are acquired with an IX81 FV1000 inverted microscope (Olympus, Hamburg, Germany). The setup allows us to image both dye channels sequentially, excluding any cross talk. We acquire the two channels in a line-wise mode, minimizing the influence of filament movement between acquisition of the two channels, which is particularly important for the investigations in the diffusion chambers. To improve image quality of static filaments adhered to glass slides, we use a Kalman filter where each frame is imaged twice to reduce image noise. A pixel dwell time of 10 ns with low laser intensity settings has proven to represent the best compromise between imaging speed and photobleaching. We use a 60×, 1.3 NA silicon oil-immersion objective (UPLSAPO 60×S; Olympus, Hamburg, Germany). In the case of the diffusion chambers, we focus on the center of the chamber to exclude surface effects and acquire an image every 5 min. MATLAB (The MathWorks, Natick, MA) scripts are used for data analysis.

RESULTS

A major challenge for the study of the exchange dynamics between fluorescently labeled protein complexes or filaments is the quantitative analysis of the fluorescence images. To approach this problem for vimentin IFs, we

employ two experimental setups: microfluidic diffusion chambers and a standard bulk scenario.

Vimentin assembly in microfluidic diffusion chambers

We perform experiments in microfluidic flow chambers to follow the assembly of vimentin in situ and by fluorescence microscopy. The chambers provide a three-dimensional confined environment in which the vimentin subunits and filaments can move freely in solution. Even though this technique does not resolve the smallest subunits, i.e., nanometer-sized tetramers, we can assess different cluster sizes as soon as they have reached microscopic resolution (few hundreds of nanometers) and thereby determine the timescales of the assembly reaction in our system.

After application of the lipid coating (see Materials and Methods), the device is flushed with 2 mM phosphate buffer for 30 min. Unassembled protein (0.4 g/L) is flushed through the main channel and enters the chambers by diffusion. The equilibration process is mostly finished after 30 min. To initiate the assembly process, 100 mM KCl in 2 mM phosphate buffer is flushed through the main channel. Because of the small diffusion coefficients of 1.9×10^{-9} m^2/s of the ions, the KCl concentration in the chamber equilibrates within a few minutes, and thus initiates the assembly of vimentin protein into filaments.

To quantify the assembly process in microfluidic diffusion chambers, we determine the standard deviation σ of the gray-scale values of the individual camera pixels within the chamber area for each image and normalize by the mean intensity μ, as illustrated in Fig. 3 *a*. We thus obtain the coefficient of variation σ/μ (CV) for each image, which is the inverse of the signal/noise. Data are normalized to 1 for each time series of identical duration and then averaged. Fig. S1 in the Supporting Material shows the relation between proceeding filament assembly and increasing CV.

As long as only small assemblies, which cannot be resolved by fluorescence microscopy, are present and homogeneously distributed, we obtain a low value for the CV. The more advanced the assembly reaction is, the more clusters of higher intensity are present and thus we observe an increasing CV. Thus, a low signal/noise—a noisy image—corresponds to the presence of filaments in the image. This data analysis method captures the transition between free subunits (smaller than the resolution limit of the employed microscopy) and larger aggregates, which can be resolved. Here, we are primarily interested in obtaining the timescale at which the earlier steps in the IF assembly occur, to compare it to the timescales for subunit exchange.

Having two differently labeled species of vimentin with identical assembly properties, we investigate whether the presence of fully grown, mature vimentin filaments influences the assembly of newly added assembly-competent tetramers. We compare the temporal evolution of the CV of vimentin assembly on its own with that of vimentin assembled in the presence of vimentin IFs (*green* and *red curve* in Fig. 3 *b*, respectively). We observe a rapid increase within the first 10 minutes and a saturation after ~1 h. Notably, the two curves practically superimpose. Hence, both curves are fitted to a limited exponential growth function, which yields a time constant of 31 min, irrespective of the dye used for labeling. The prior presence of green filaments does not influence the assembly of red filaments. We can thus be certain that after 1 h the available protein is mostly incorporated into filaments and free subunits, which are not resolved in fluorescence microscopy, only occur in the context of subunit exchange between filaments. The observed timescales are in accordance with previous results from small-angle x-ray scattering, electron microscopy, and

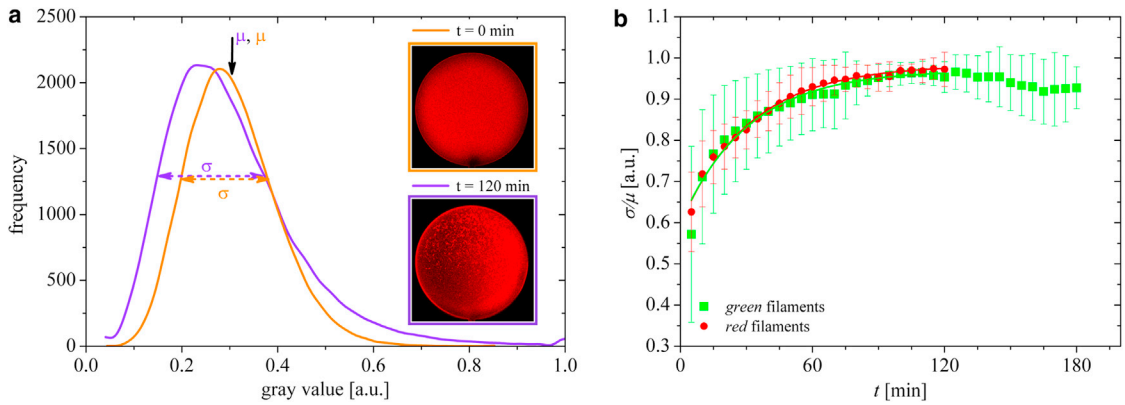

FIGURE 3 Assembly kinetics observed in diffusion chambers. (*a*) The normalized, smoothed gray values at $t = 0$ min are distributed around the mean μ with a standard deviation σ. For $t = 120$ min, σ increases. (*Insets*) Typical images at the two different time points. For $t = 120$ min, filaments are observed. Chamber diameter shown here is 200 μm. (*b*) Temporal evolution of filament growth is indicated by an increasing coefficient of variation σ/μ in the microscopy images. An exponential fit of the first 120 min (*solid lines*) yields a time constant τ of 31 min. Behavior for assembly of only green filaments (*squares*) and the assembly of red filaments in the presence of preassembled green filaments (*circles*) is identical. Error bars are standard deviations. To see this figure in color, go online.

atomic-force microscopy studies, where after a few minutes the filament lengths are in the range of the optical resolution (15,16,38).

Investigation of subunit exchange in bulk experiments

In parallel to the assembly reaction as described in the previous paragraph, the specific architecture of vimentin IFs opens up the possibility for release and incorporation of subunits from fully assembled filaments without compromising their stability. As a starting point for experiments, which we designed to test this hypothesis, assembly of vimentin filaments is performed in two different manners (11) and separately for differently labeled filaments, as follows.

Set A: To obtain filaments with uniform cross-section, assembly of vimentin (0.2 g/L) is performed by dialysis into 2 mM phosphate buffer, pH 7.5, 100 mM KCl.

Set B: Filaments with a pronounced polymorphism with respect to the number of tetramers per filament cross-section are assembled in a kick-start mode by mixing vimentin (0.4 g/L) in 2 mM phosphate buffer, pH 7.5 with an equal volume of 2 mM phosphate buffer, pH 7.5 containing 200 mM KCl (11).

In both cases, assembly is performed at 37°C for at least 12 h. Thus, with regard to the results from in situ assembly experiments, we ensure that we obtain long and easily visible filaments as well as a small amount of free subunits.

Three different experiments (see Table 1 for an overview of the experimental conditions) are performed with these filaments, as follows.

Method I: Red tetrameric vimentin (0.6 g/L) is mixed with an equal volume of 2 mM phosphate buffer, pH 7.5, 200 mM KCl (39). Immediately after, we mix this solution with an equal volume of green filaments (0.2 g/L) assembled in a reaction tube (Set B).

Method II: Red tetrameric vimentin (0.4 g/L) is mixed with an equal volume of 2 mM phosphate buffer, pH 7.5, 200 mM KCl. Immediately after, we mix this solution with an equal volume of green filaments (0.2 g/L) assembled by dialysis (Set A).

Method III: Red and green vimentin filaments (0.2 g/L) assembled by dialysis are mixed (Set A/Set A), resulting in a final concentration of 0.1 g/L of each filament type (final–final).

In all three cases, solutions are incubated at 37°C and samples are taken every 60 min. The assembly and subunit exchange reactions are stopped by 20-fold dilution with assembly buffer. For imaging, 5 μL sample solution are placed on a glass slide, to which filaments and smaller aggregates adhere within 1 min.

In the following, filaments labeled with AlexaFluor 488, which are present in filamentous form at the beginning of each experiment, are referred to as "green filaments". Vimentin labeled with Atto 647N, which is introduced in tetrameric form or as already assembled filaments, is referred to as either "red vimentin" or "red filaments". In our setting, the red filaments are the donors and the green filaments are the acceptors.

We observe end-to-end annealing, as previously reported in vitro (18), and in cells (29) (see *arrow 1* in Fig. 4) and regions where red and green filaments overlap (*arrow 2*), which are excluded from the analysis. Capping of green filaments by red subunits (probably one ULF, or several ULFs) is also frequently observed when adding red tetrameric vimentin to green preassembled filaments (Fig. 4, panels II, *top-left corner*). Additionally, however, we find a red signal at the position of the green filaments (*arrow 3*), which corresponds to exchanged subunits. We assume that this red signal corresponds to tetramers or multiples thereof, but not complete ULFs because we observe green filaments with red spots rather than striped filaments. To quantify these observations, the average intensity I_{fil} of all red filaments in a single image is calculated. The average red intensity I_{ex} for each image at the position of the green filaments is identified as the position of exchanged red subunits. The background in the red channel is subtracted from each of these values and the relative amount of exchanged subunits $A = I_{\mathrm{ex}}/I_{\mathrm{fil}} \times 100$ is calculated.

The use of I_{fil} as a reference value for the amount of exchanged subunits introduces a small error into the results and $I_{\mathrm{fil}} + I_{\mathrm{ex,green}}$ would be more precise. However, because it is not possible to determine $I_{\mathrm{ex,green}}$ accurately, we have estimated the maximum absolute error for A to be in the range of 1% and therefore we can neglect it. In Fig. 5 *a*, we show data for the experimental conditions I–III. Additionally, data sets at higher temporal resolution (15 min) and therefore including early time points at the expense of statistics are taken (see Fig. 5 *b*). We identify three phases in the subunit exchange. Within the first hour, the percentage of exchanged subunits increases fast and possibly exponentially while the fluorescent background decreases and remains stable at a low level after ~60 min. This finding

TABLE 1 Overview of the different experimental conditions used for the experiments shown in Figs. 4 and 5

	Experimental method I	Experimental method II	Experimental method III
Red	Tetramers (0.3 g/L)	Tetramers (0.2 g/L)	Uniform (Set A, 0.2 g/L)
Green	Polymorphic (Set B, 0.2 g/L)	Uniform (Set A, 0.2 g/L)	Uniform (Set A, 0.2 g/L)
Final protein concentration	0.25 g/L	0.2 g/L	0.2 g/L

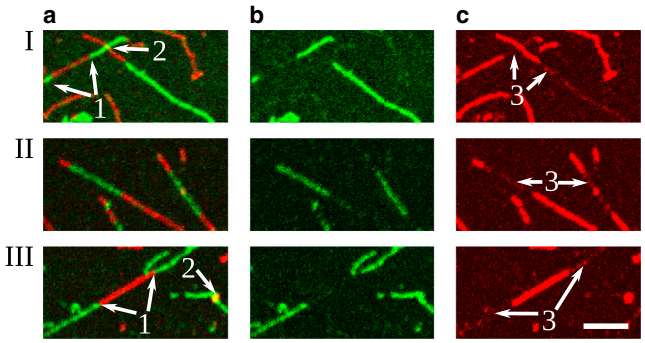

FIGURE 4 Fluorescent images of vimentin filaments 5 h after initiation of the experiment. Note that the filaments are stretched out on glass slides and therefore appear less curvy than their persistence length would suggest. (*a*) Merged red and green channels; (*b*) green channel; (*c*) red channel. Image brightness in panel *c* (but not in panel *a*) is adjusted for maximal visibility of exchanged subunits. Different experimental conditions are as follows: I, red subunits mixed with green polymorphic filaments; II, red subunits mixed with green uniform filaments; III, red and green uniform filaments mixed together. (*Arrow 1*) End-to-end annealing; (*arrow 2*) overlapping filaments (these regions are excluded from the analysis); (*arrow 3*) exchanged subunits (scale bar, 2 μm). To see this figure in color, go online.

indicates that the number of incorporated subunits is proportional to the number of soluble subunits, which decreases over time, and we obtain a growth law of the form $dA(t)/dt = \kappa^{-1}(A_\infty - A(t))$. This assumption is further supported by the observation that for experimental condition III, where fully assembled red and green filaments are mixed, this fast increase in $A(t)$ for early times is not observed.

Between 60 min and ~420 min the increase continues, yet at a slower rate and can roughly be characterized by a linear law, $A(t) = a_j t + B$ with a constant offset B, where the slope a_j is different for the different experimental conditions. We observe the same behavior when red and green fluorophores are interchanged and can thus exclude an effect of the labels. For the three specific experimental conditions, we obtain $a_{\mathrm{I}} = 0.95 \pm 0.09\%/\mathrm{h}$, $a_{\mathrm{II}} = 0.68 \pm 0.10\%/\mathrm{h}$, and $a_{\mathrm{III}} = 0.34 \pm 0.06\%/\mathrm{h}$. Thus, the subunit exchange rates for the addition of tetrameric vimentin to polymorphic acceptor filaments (I) is fastest, followed by the rates for the addition of tetrameric vimentin to smooth acceptor filaments (II). A smaller value is observed when assembled filaments are combined (III). With these rates, we find a total amount of exchanged subunits of ~10% after 7 h for Methods I and II. For longer times (23–26 h), $A(t)$ remains constant or increases little (for data, see Fig. S2). The slightly higher protein concentration for Method I (see Table 1) only influences the red filament assembly and competing subunit exchange in the first hour, but not the observed rates at later times. The implications of the submaximal saturation at a few percent exchanged subunits could be that an equilibrium between incorporation of red subunits into green filaments and vice versa has been reached. Moreover, most likely only subunits located at the outside of the filament are released and new subunits are included at these sites as well, because the other subunits are more strongly bound to the filament. Given a standard number of eight tetramers per cross-section and assuming the tetramer as the smallest exchangeable subunit, only one to very few tetramers per ULF are exchanged. Note, however, that the system is by no means static, but instead reaches a steady state after a certain time.

DISCUSSION

IFs exhibit a remarkable polymorphism with respect to the number of subunits per cross-section (4). In particular,

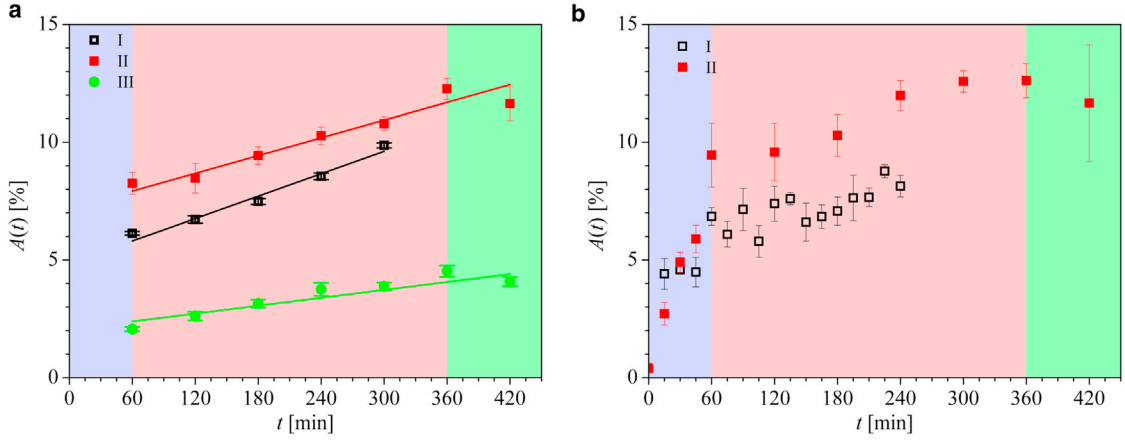

FIGURE 5 (*a*) For each experimental method (I–III), the percentage of exchanged subunits $A(t)$ is averaged for each experimental day (2–7) first and then between the experimental days (including a total 22–72 images per data point shown here). $A(t)$ increases over time and saturates after ~6 h. Different experimental conditions are as follows: I, red subunits mixed with green polymorphic filaments; II, red subunits mixed with green uniform filaments; III, red and green uniform filaments mixed together. Error bars are standard deviation from the individual images for each experimental day and error propagation to combine the experimental days. (*b*) During the first phase (first hour in our experiment) of subunit exchange, we observe a fast increase of $A(t)$, followed by a linear increase (second phase) for later times. Shown are individual experimental days including 2–24 images per data point. Error bars are standard deviation from the individual images. To see this figure in color, go online.

when the assembly process is started through instantaneous rise of the ionic strength (kinetic mode), vimentin filaments exhibit a striking variation in the number of subunits per cross-section with peak values translating into 32, 40, and 48 molecules. This kind of polymorphism is not as drastic when filaments are assembled by dialysis from tetramer conditions into assembly conditions (11). Consequently, polymorphic filaments may be subject to a significant subunit exchange process. Notably, this polymorphism has also been observed for other IF proteins such as desmin, neurofilament proteins, and various keratins. It also appears to be a general property of cytoplasmic IFs, which may be the cause for unique functional features of IFs (13,23,25).

We now test this hypothesis by comparing experiments performed with filaments of different degrees of polymorphism. We observe the lowest exchange rate $a_{\mathrm{III}} = 0.34\%$/h when both the donor and acceptor filaments have been preassembled by dialysis and thus have a homogeneous cross-section (11). Note that this number corresponds to ~6 tetramers per hour along an average 10-μm filament. This highlights the sensitivity of the employed detection methods but also shows that interfilament subunit exchange represents a slow mechanism compared to hierarchical filament assembly. The slow subunit exchange also implies that the amount of free subunits at any given time point is small. If only the acceptor filaments are generated by dialysis and nonassembled tetramers are added, the exchange rate increases from this ground state to $a_{\mathrm{II}} = 0.68\%$/h. Moreover, for polymorphic acceptor filaments and added tetramers, it increases even more to $a_1 = 0.95\%$/h.

We thus conclude that the most pronounced exchange of subunits occurs when both donor and acceptor filaments show cross-section polymorphism. Regarding the donor filaments, a possible interpretation of these findings is that increased polymorphism leads to a looser binding of the subunits in the filaments; i.e., there are more unsaturated binding sites, where stabilization through longitudinal fixation is missing, and therefore the subunits are more likely released and available for incorporation into the acceptor filament. According to our data, for the acceptor filament, this increased number of available binding sites leads to a more probable incorporation. For cells, Colakoğlu and Brown (29) have proposed the term "intercalary subunit exchange", meaning the release and incorporation of subunits at distinct sites along the filaments. We can now refine this model by including the influence of polymorphism along the length of the assembled filaments.

Vimentin IFs can incorporate subunits in two ways. The primary mechanism is the elongation of the filament by addition of subunits in a hierarchical manner via ULFs. The second mechanism, which we have investigated in this study, is the incorporation of subunits into the bulk of the filament. Notably, the structure of the vimentin IFs remains stable, even though subunits are temporarily removed for exchange. Thus, two competing reactions are occurring and it is insightful to have a closer look at the involved timescales. Formation of ULFs from tetramers takes place within a few seconds (15) and filaments are formed within minutes (16,38). Elongation levels off by 1 h but continues, although much more slowly, through longitudinal annealing of long filaments, as shown by total internal reflection fluorescence microscopy of fluorescently labeled vimentin (18).

Notably, as we have shown in this study, subunit incorporation takes place in parallel and continues constantly. Thus, within the first hour, if unassembled vimentin is present, both reactions occur. The subunit exchange is slowed down by the decreased availability of subunits, and proceeds at a constant rate defined by those subunits that are released from fully assembled filaments and subsequently incorporated. An important conclusion from this work is, however, that whereas the subunit exchange in assembled filaments can be measured by sensitive detection techniques, it is a slow process, and for many of the existing studies does not necessarily have to be taken into account. This is in strong contrast to, e.g., the ability of actin filaments to very dynamically polymerize and depolymerize if not chemically stabilized.

The exchange of subunits could have implications for the properties of the filaments and the cytoskeleton as a whole. The polymorphism, which as we have shown here is closely linked to loss and incorporation of subunits, most likely leads to varying mechanical properties of the filaments and may also allow for the binding of different types of associated proteins and their complexes. It is unclear whether the subunit exchange leads to smoother filaments over time, i.e., whether thicker filament sections are more likely to lose subunits and thinner sections accept them more easily. In the cell, this phenomenon could be controlled by locally increasing or decreasing the amount of subunits in the soluble pool or through regulation of protein-kinase activity. Furthermore, the subunit exchange mechanism could be relevant during differentiation of cells, which can be related to network rearrangements or a switch in IF types.

Compared to the in vitro system described here, the situation in the cell is obviously much more complex, with many more unknowns; therefore, a direct comparison of our results to literature data from cell experiments cannot be straightforward. Furthermore, the work in Colakoğlu and Brown (29) used fluorescent fusion proteins whereas we employ labeling with small synthetic dyes. Potentially, the larger size of the fusion proteins could lead to a more polymorphic and less tightly bound state, in turn leading to more pronounced subunit exchange. Despite these differences, we can set the amount of subunits with the donor label incorporated into the acceptor filament into perspective: In the cellular system, the authors find an exchange of fluorescence intensity of ~10% after 8 h (29), while we find between 4 and 10% depending on the polymorphism of the filaments. Hence, the similarity to our results might indicate that, despite regulatory mechanisms in the cell,

subunit exchange may occur due to this inherent property of IF proteins exhibited by vimentin and the neurofilament proteins. Notably, a small amount of free vimentin tetramers has been identified in different fibroblast cell lines early on by biochemical methods (40). Accordingly, Soellner et al. (40) have concluded: "We propose that in the living cell a small pool of a distinct soluble tetrameric form of vimentin exists which may exchange with polymeric IF vimentin."

SUPPORTING MATERIAL

Two figures are available at http://www.biophysj.org/biophysj/supplemental/S0006-3495(14)01137-0.

We thank Norbert Mücke and Stefan Winheim for technical help, Edith Schäfer and Andreas Janshoff for assistance with the lipid bilayer coating, and Susanne Bauch for the preparation of vimentin protein.

We acknowledge funding from the Deutsche Forschungsgemeinschaft (DFG) through the Cluster of Excellence and DFG Research Center Nanoscale Microscopy and Molecular Physiology of the Brain, the Excellence Initiative, the project No. KO 3752/5-1/HE 1853/11-1, HE 1853/11-1, and HE 1853/9-2, and the collaborative research center SFB 755 (Nanoscale Photonic Imaging), project No. B07.

REFERENCES

1. Kasza, K. E., A. C. Rowat, …, D. A. Weitz. 2007. The cell as a material. *Curr. Opin. Cell Biol.* 19:101–107.
2. Janmey, P. A., and C. A. McCulloch. 2007. Cell mechanics: integrating cell responses to mechanical stimuli. *Annu. Rev. Biomed. Eng.* 9:1–34.
3. Fuchs, E., and I. Karakesisoglou. 2001. Bridging cytoskeletal intersections. *Genes Dev.* 15:1–14.
4. Parry, D. A. D., and P. M. Steinert. 1995. Intermediate Filament Structure. CRC Press, Boca Raton, FL.
5. Herrmann, H., and U. Aebi. 2004. Intermediate filaments: molecular structure, assembly mechanism, and integration into functionally distinct intracellular scaffolds. *Annu. Rev. Biochem.* 73:749–789.
6. Guo, M., A. J. Ehrlicher, …, D. A. Weitz. 2013. The role of vimentin intermediate filaments in cortical and cytoplasmic mechanics. *Biophys. J.* 105:1562–1568.
7. Seltmann, K., A. W. Fritsch, …, T. M. Magin. 2013. Keratins significantly contribute to cell stiffness and impact invasive behavior. *Proc. Natl. Acad. Sci. USA.* 110:18507–18512.
8. Herrmann, H., S. V. Strelkov, …, U. Aebi. 2009. Intermediate filaments: primary determinants of cell architecture and plasticity. *J. Clin. Invest.* 119:1772–1783.
9. Mendez, M. G., S. Kojima, and R. D. Goldman. 2010. Vimentin induces changes in cell shape, motility, and adhesion during the epithelial to mesenchymal transition. *FASEB J.* 24:1838–1851.
10. Iwatsuki, H., and M. Suda. 2010. Seven kinds of intermediate filament networks in the cytoplasm of polarized cells: structure and function. *Acta Histochem. Cytochem.* 43:19–31.
11. Herrmann, H., M. Häner, …, U. Aebi. 1996. Structure and assembly properties of the intermediate filament protein vimentin: the role of its head, rod and tail domains. *J. Mol. Biol.* 264:933–953.
12. Herrmann, H., and U. Aebi. 1998. Intermediate filament assembly: fibrillogenesis is driven by decisive dimer-dimer interactions. *Curr. Opin. Struct. Biol.* 8:177–185.
13. Herrmann, H., M. Häner, …, U. Aebi. 1999. Characterization of distinct early assembly units of different intermediate filament proteins. *J. Mol. Biol.* 286:1403–1420.
14. Sokolova, A. V., L. Kreplak, …, S. V. Strelkov. 2006. Monitoring intermediate filament assembly by small-angle x-ray scattering reveals the molecular architecture of assembly intermediates. *Proc. Natl. Acad. Sci. USA.* 103:16206–16211.
15. Brennich, M. E., J.-F. Nolting, …, S. Köster. 2011. Dynamics of intermediate filament assembly followed in micro-flow by small angle x-ray scattering. *Lab Chip.* 11:708–716.
16. Kirmse, R., S. Portet, …, J. Langowski. 2007. A quantitative kinetic model for the in vitro assembly of intermediate filaments from tetrameric vimentin. *J. Biol. Chem.* 282:18563–18572.
17. Portet, S., N. Mücke, …, H. Herrmann. 2009. Vimentin intermediate filament formation: in vitro measurement and mathematical modeling of the filament length distribution during assembly. *Langmuir.* 25: 8817–8823.
18. Winheim, S., A. R. Hieb, …, N. Mücke. 2011. Deconstructing the late phase of vimentin assembly by total internal reflection fluorescence microscopy (TIRFM). *PLoS ONE.* 6:e19202.
19. Fraser, R. D. B., T. P. MacRae, …, D. A. D. Parry. 1985. Intermediate filament structure: 2. Molecular interactions in the filament. *Int. J. Biol. Macromol.* 7:258–274.
20. Kreplak, L., H. Bär, …, U. Aebi. 2005. Exploring the mechanical behavior of single intermediate filaments. *J. Mol. Biol.* 354:569–577.
21. Starger, J. M., W. E. Brown, …, R. D. Goldman. 1978. Biochemical and immunological analysis of rapidly purified 10-nm filaments from baby hamster kidney (BHK-21) cells. *J. Cell Biol.* 78:93–109.
22. Steven, A. C., J. Wall, …, P. M. Steinert. 1982. Structure of fibroblastic intermediate filaments: analysis of scanning transmission electron microscopy. *Proc. Natl. Acad. Sci. USA.* 79:3101–3105.
23. Steven, A. C., J. F. Hainfeld, …, P. M. Steinert. 1983. The distribution of mass in heteropolymer intermediate filaments assembled in vitro. Stem analysis of vimentin/desmin and bovine epidermal keratin. *J. Biol. Chem.* 258:8323–8329.
24. Eichner, R., P. Rew, …, U. Aebi. 1985. Human epidermal keratin filaments: studies on their structure and assembly. *Ann. N. Y. Acad. Sci.* 455:381–402.
25. Engel, A., R. Eichner, and U. Aebi. 1985. Polymorphism of reconstituted human epidermal keratin filaments: determination of their mass-per-length and width by scanning transmission electron microscopy (STEM). *J. Ultrastruct. Res.* 90:323–335.
26. Ngai, J., T. R. Coleman, and E. Lazarides. 1990. Localization of newly synthesized vimentin subunits reveals a novel mechanism of intermediate filament assembly. *Cell.* 60:415–427.
27. Vikstrom, K. L., G. G. Borisy, and R. D. Goldman. 1989. Dynamic aspects of intermediate filament networks in BHK-21 cells. *Proc. Natl. Acad. Sci. USA.* 86:549–553.
28. Vikstrom, K. L., S.-S. Lim, …, G. G. Borisy. 1992. Steady state dynamics of intermediate filament networks. *J. Cell Biol.* 118:121–129.
29. Colakoğlu, G., and A. Brown. 2009. Intermediate filaments exchange subunits along their length and elongate by end-to-end annealing. *J. Cell Biol.* 185:769–777.
30. Eriksson, J. E., T. He, …, R. D. Goldman. 2004. Specific in vivo phosphorylation sites determine the assembly dynamics of vimentin intermediate filaments. *J. Cell Sci.* 117:919–932.
31. Chou, Y.-H., S. Khuon, …, R. D. Goldman. 2003. Nestin promotes the phosphorylation-dependent disassembly of vimentin intermediate filaments during mitosis. *Mol. Biol. Cell.* 14:1468–1478.
32. Heins, S., and U. Aebi. 1994. Making heads and tails of intermediate filament assembly, dynamics and networks. *Curr. Opin. Cell Biol.* 6:25–33.
33. Herrmann, H., L. Kreplak, and U. Aebi. 2004. Isolation, characterization, and in vitro assembly of intermediate filaments. *Methods Cell Biol.* 78:3–24.

34. Deshpande, S., and T. Pfohl. 2012. Hierarchical self-assembly of actin in micro-confinements using microfluidics. *Biomicrofluidics.* 6:34120.

35. Xia, Y., and G. M. Whitesides. 1998. Soft lithography. *Annu. Rev. Mater. Sci.* 28:153–184.

36. Yang, T., S. Jung, …, P. S. Cremer. 2001. Fabrication of phospholipid bilayer-coated microchannels for on-chip immunoassays. *Anal. Chem.* 73:165–169.

37. Persson, F., J. Fritzsche, …, J. O. Tegenfeldt. 2012. Lipid-based passivation in nanofluidics. *Nano Lett.* 12:2260–2265.

38. Czeisler, E., A. Mizera, …, I. Petre. 2012. Quantitative analysis of the self-assembly strategies of intermediate filaments from tetrameric vimentin. *IEEE-ACM Trans. Comput. Biol.* 9:885–898.

39. Mücke, N., L. Kreplak, …, J. Langowski. 2004. Assessing the flexibility of intermediate filaments by atomic force microscopy. *J. Mol. Biol.* 335:1241–1250.

40. Soellner, P., R. A. Quinlan, and W. W. Franke. 1985. Identification of a distinct soluble subunit of an intermediate filament protein: tetrameric vimentin from living cells. *Proc. Natl. Acad. Sci. USA.* 82:7929–7933.